

## A meta-stacking ensemble framework for landslide susceptibility mapping using LightGBM, Histogram Gradient Boosting and Decision Tree

Alireza Habibi Khouzani <sup>1\*</sup>, Mahmoud Reza Delavar <sup>1,2</sup>, Armin Moghimi <sup>3</sup>, Chiranjit Singha <sup>4</sup>, Mir Abolfazl Mostafavi <sup>5</sup>

<sup>1</sup> School of Surveying and Geospatial Engineering, College of Engineering, University of Tehran – Tehran, Iran, (Email: mo.alireza77habibi@gmail.com, mdelavar@ut.ac.ir)

<sup>2</sup> Center of Excellence in Geomatic Eng. in Disaster Management and Land Administration in Smart City Lab., School of Surveying and Geospatial Eng., College of Engineering, University of Tehran, Tehran P.O. Box 14155-6619, Iran,

<sup>3</sup> Department of Photogrammetry and Remote Sensing, Geomatics Engineering Faculty, K. N. Toosi University of Technology, Tehran, Iran, (Email: moghimi@kntu.ac.ir, moghimi.armin@gmail.com)

<sup>4</sup> Department of Agricultural Engineering, Institute of Agriculture, Visva-Bharati (A Central University), Sriniketan, Birbhum, 731236, West Bengal, India, (Email: singha.chiranjit@gmail.com)

<sup>5</sup> Center of Research in Geospatial Data and Intelligence, Department of Geomatics Sciences, Université Laval, 1055, Avenue du Séminaire, Quebec City, QC, Canada, (Email: mir-abolfazl.mostafavi@scg.ulaval.ca)

**KEY WORDS:** Landslide susceptibility mapping, Meta-stacking ensemble, LightGBM, Gradient boosting; Decision tree, GIS uncertainty assessment

### ABSTRACT:

Landslides are a major natural hazard in mountainous regions, causing substantial socio-economic losses and posing persistent threats to infrastructure and human safety. This study introduces a Meta-Stacking Ensemble model for advanced landslide susceptibility mapping in the Darjeeling Himalayas, India. The proposed framework integrates LightGBM, Histogram Gradient Boosting, and Decision Tree algorithms through a stacking approach that maintains the original geospatial features while enhancing ensemble diversity. In this way, fourteen key conditioning factors (i.e., topographic, geological, hydrological and anthropogenic variables) were analyzed. Validation using 1830 landslide polygons demonstrated the model's superior predictive performance, achieving an AUC of 0.93, overall accuracy of 87%, Recall of 0.84 and F1-score of 0.72, outperforming all individual base models. Spatial analysis indicated that 22% of the area falls within the "Very High" risk zone, with slope gradient (28% importance) and proximity to tectonic faults (30%) identified as dominant controlling factors. The developed framework produces GIS-compatible susceptibility maps with quantified uncertainty metrics, providing valuable insights to support disaster risk management and mitigation planning.

### 1. INTRODUCTION

Landslides rank among the most recurrent and destructive natural hazards, causing severe socio-economic losses and posing persistent threats to human lives and infrastructure (Biswas et al., 2023; Gupta et al., 2021). Their mechanisms such as rock falls, debris slides, and block slides (Agboola et al., 2024), vary widely and are influenced by factors including geology, rainfall, seismic activity, and topography (Barman et al., 2022a; Basharat et al., 2023; Yi et al., 2020). Mountainous regions worldwide are particularly vulnerable, where recurrent landslides disrupt communities and impede sustainable development. The Himalayas exemplify this challenge, experiencing frequent and devastating events that heavily impact both the environment and human settlements (Barman et al., 2022b; Gupta and Shukla, 2022; Peethambaran et al., 2018).

In the Darjeeling Himalayas (covering Kalimpong and Darjeeling districts) intense monsoons and seismic activity frequently trigger landslides, leading to catastrophic losses (Bera et al., 2021; Sumantra and Raghunath, 2016). For instance, during June–July 2015, landslides claimed 38 lives and left 23 missing across towns such as Kurseong, Mirik and Darjeeling (Sumantra and Raghunath, 2016). These recurring disasters highlight the urgent need for proactive risk mitigation and coordinated efforts among governmental and private agencies (Habibi et al., 2023b, 2023a).

Landslide Susceptibility Mapping (LSM) has become a key tool for hazard assessment, integrating geo-environmental variables such as lithology, elevation, land use/land cover (LULC), and

climate (Lee et al., 2017; Saha et al., 2021; Sonker et al., 2021; Yi et al., 2022; Youssef et al., 2022; Zhang et al., 2022; Zhu et al., 2020). While traditional statistical approaches (e.g. Index of Entropy [IOE]), have proven useful (Jakob, 2022; Naceur et al., 2022), recent advances combine Machine Learning (ML), Deep Learning (DL), Geospatial Information Systems (GIS), and Remote Sensing (RS) to achieve higher predictive accuracy (Habibi et al., 2023a).

Recent advances in ML have transformed LSM capabilities, with ensemble methods like Random Forest (RF) achieving 89% prediction accuracy in Uttarakhand and DL models like Convolutional Neural Networks (CNNs) reaching 97% Area Under the Curve (AUC) in China (Farhadi et al., 2022; Saha et al., 2023). However, these approaches face key challenges in Himalayan contexts. First, traditional stacking ensembles often discard original geo-environmental features during meta-learning, eliminating valuable spatial information. Second, the frequent use of similar base model architectures leads to correlated errors and reduced ensemble diversity. Third, DL models demand high computational resources, limiting their feasibility in data- and hardware-constrained regions.

To address these methodological and contextual constraints, the present study introduces an improved ensemble learning framework specifically tailored to complex mountainous environments. This study proposes a Meta-Stacking Ensemble model that overcomes these limitations through an innovative architecture. It employs a dual-channel feature integration system that preserves original geo-environmental variables while

\* Corresponding author

incorporating base model probabilities, retaining spatial detail typically lost in conventional stacking. The ensemble combines LightGBM (max\_depth=3), L2-regularized Histogram Gradient Boosting (max\_leaf\_nodes=15), and a Decision Tree (min\_samples\_split=20)—selected to maximize error diversity. An enhanced preprocessing pipeline also applies iterative multivariate imputation and Spearman correlation-based feature selection to ensure robustness under Himalayan data constraints.

## 2. DATA AND METHODS

### 2.1 Study area

The study area covers the geologically dynamic Darjeeling and Kurseong districts of West Bengal, India (26°07'74"N–27°02'21"N, 88°00'09"E–88°04'55"E), spanning about 1,190 km<sup>2</sup> in the eastern Himalayan foothills (Figures 1 and 2). Marked by sharp topographic variation, elevations range from 127 m in the plains to 3,600 m in the highlands, with slope angles reaching 62° in the most dissected zones. The region experiences a tropical monsoon climate with a mean annual rainfall of 600 mm, nearly 80% of which falls during June–August (Starkel and Basu, 2000). Intense rainfall events exceeding 300 mm have historically triggered numerous shallow landslides, including major occurrences in 1899, 1934, 1950, 1968, 1993, 2009, 2011, and 2015 (Banerjee et al., 2022; Sarkar et al., 2013).

Geologically, the study area comprises a complex assemblage of Permian, Precambrian, and Miocene formations (Pawde and Saha, 1982) within the tectonically active Gorubathan and Rangamati zones. The region exhibits six major landform units: (1) alluvial plains, (2) piedmont fans, (3) active floodplains, (4) folded ridges, (5) intermontane valleys, and (6) highly dissected hill slopes (Chawla et al., 2019). Soil textures vary systematically with topography, ranging from fine-loamy compositions in valley bottoms to gravelly loamy and coarse-loamy types on steeper slopes, reflecting the interplay of weathering processes and slope dynamics.

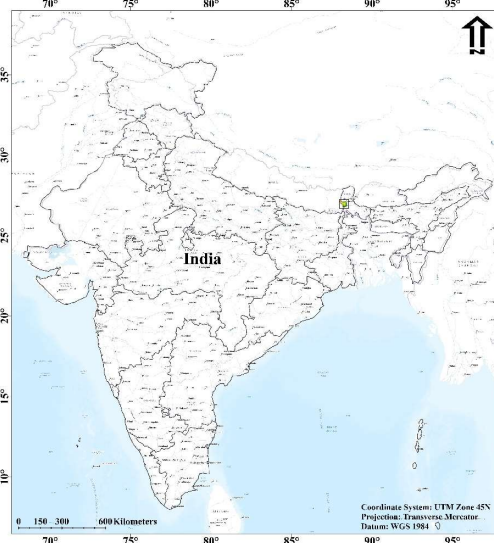


**Figure 1.** Geographical setting of the study area in Darjeeling Himalayas, India.

### 2.2 Method

A total of 1830 landslide polygons were mapped using multi-source data from Bhuvan NRSC, Google Earth imagery (2010–2022), and GSI records, showing significant size variation (8.70–234,699 m<sup>2</sup>, median=312.56 m<sup>2</sup>, CV=3.72). The inventory

predominantly contains debris slides (62%), rockfalls (28%), and soil accumulation slides (10%), verified through field surveys with ±10 m DGPS accuracy. These were converted to binary data (landslide/non-landslide) and split into 70% training and 30% testing datasets using stratified sampling, with non-landslide points selected from stable areas with matching terrain characteristics (Figure 3). The final dataset comprised 1,309 landslide points and an equal number (1,309) of non-landslide points.

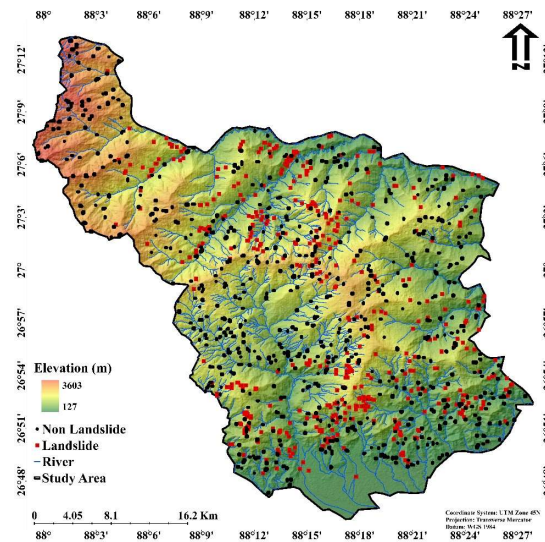


**Figure 2.** Geographical setting of the study area in Darjeeling Himalayas, India, with elevation gradient and landslide and non-landslide points.

### 2.3 Data used

Developing a reliable Landslide Susceptibility Map (LSM) required constructing a Landslide Inventory Map (LIM) from historical landslide and non-landslide locations and analyzing spatial relationships between landslide occurrences and causative factors. Guided by data availability, the region's geo-environmental characteristics, and prior studies (Moghimi et al., 2024), fourteen influencing factors were integrated into the model including elevation, Sediment Transport Index (STI), earthquakes, slope, aspect, lineament density, distance to fault, soil erosion, distance to river, Global Human Modification (GHM), soil type, precipitation, NDVI, and distance to road (Figure 4), with their spatial correlations systematically evaluated to inform susceptibility mapping. The employed data area as follows:

#### 2.3.1 Topographic Factors

Elevation (SRTM DEM, 30 m resolution) influences landslide susceptibility by affecting gravitational stress, weathering rates, and hydrological processes. Higher elevations often exhibit steeper slopes and unstable geological formations. Slope (degrees) directly governs shear stress, with steeper slopes being more prone to failures. Aspect (direction of slope face) impacts soil moisture retention and vegetation cover, indirectly altering slope stability. STI, derived from slope and flow accumulation, quantifies erosional energy, highlighting areas with high sediment mobility (Habibi et al., 2023; Habibi et al., 2022; Saha et al., 2023).

#### 2.3.2 Geological and Seismic Factors

Earthquakes (Geological Survey of India data) trigger landslides by generating ground shaking that reduces shear strength in slopes. Lineament density (km/km<sup>2</sup>), calculated using ArcGIS

line density tool, indicates fracture zones prone to instability. Distance to fault (m) measures proximity to tectonic activity,

with closer distances correlating to higher landslide risk due to weakened rock structures (Shao and Xu, 2022).

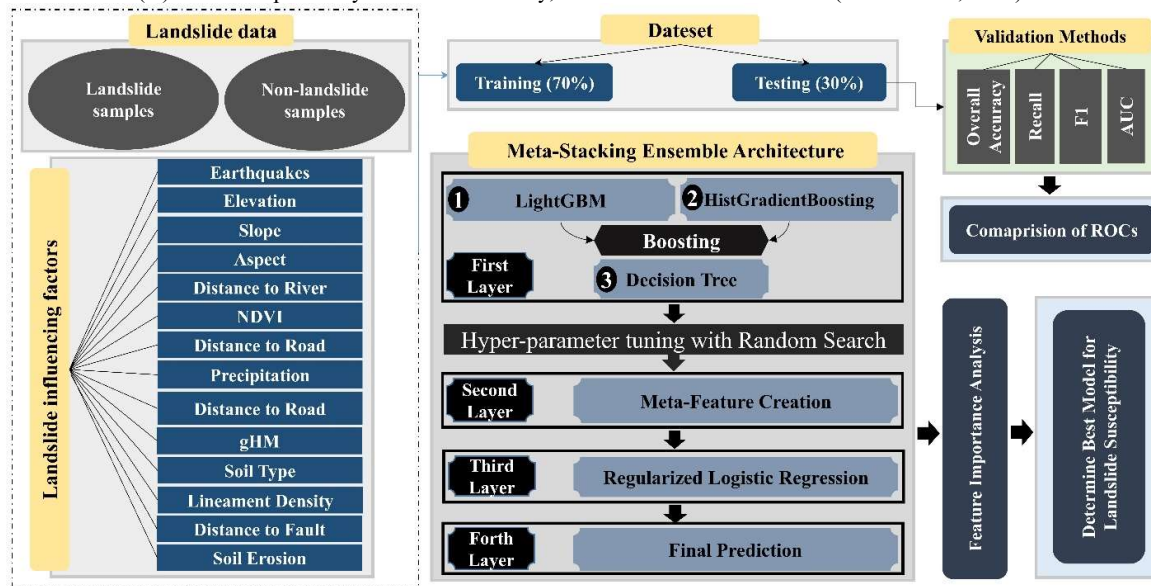


Figure 3. Research methodology.

### 2.3.3 Hydrological and Climatic Factors

Precipitation (CHIRPS v2.0, 1981–2022) saturates slopes, increasing pore pressure and reducing soil cohesion. Distance to river (HydroSHEDS) reflects fluvial erosion potential, as river undercutting destabilizes adjacent slopes (Höge et al., 2022).

### 2.3.4 Soil and Vegetation Factors

Soil type (Harmonized World Soil Database) affects permeability and shear strength, with clay-rich soils being more unstable. Soil erosion (ESDAC, tons/acre/year) indicates surface degradation, exacerbating slope failures. Normalized Difference Vegetation Index (NDVI) (Sentinel-2, 10 m) measures vegetation health, where dense root systems enhance slope stability through soil binding (Csáfordi et al., 2012).

### 2.3.5 Anthropogenic Factors

GHM (1 km resolution) aggregates human infrastructure impacts, such as deforestation and construction, which destabilize slopes. Distance to road (Open Street Map (OSM)) highlights areas where excavation and vibration from traffic increase landslide likelihood (Chu et al., 2020).

## 2.4 Machine learning models

This study employs a tiered ML framework, combining base models with a meta-stacking ensemble to predict landslide susceptibility. The architecture addresses spatial heterogeneity through algorithmic diversity and learned model weighting (Figure 3).

### 2.4.1 Light Gradient Boosting Machine

The Light Gradient Boosting Machine (LightGBM) is an advanced gradient boosting framework that efficiently handles large-scale data through its gradient-based optimization algorithm (Kim et al., 2023). The model employs a tree-based learning strategy where each subsequent tree attempts to correct the errors of previous trees, leading to progressively better predictions. In our implementation, we utilize LightGBM with balanced class weights and shallow trees ( $\text{max\_depth}=3$ ) to prevent overfitting while maintaining robust performance across classes.

### 2.4.2 Histogram Gradient Boosting

Histogram Gradient Boosting implements an efficient gradient boosting algorithm that stores feature values in histograms during training [pml.cs.wisc.edu/hgbm/](https://pml.cs.wisc.edu/hgbm/). This approach enables fast computation of optimum split points without sorting the data, making it particularly effective for handling continuous features. Our implementation employs early stopping prevention and controlled depth ( $\text{max\_depth}=3$ ) to maintain model stability.

### 2.4.3 Decision Tree

The DT acts as a foundational classifier, partitioning the feature space through recursive splits. Configured with a maximum depth of 5 and higher minimum sample splits, it minimizes overfitting. In the Meta-Stacking Ensemble (Figure 3), DT outputs, along with other base model probabilities, are merged with original features to form meta-features, which are finally processed by a regularized logistic regression meta-model for prediction.

### 2.4.4 Proposed Meta-Stacking Ensemble Architecture

The novel meta-stacking ensemble architecture implements a hierarchical learning approach that strategically combines base model predictions through three key stages. First, independent feature processing is performed by LightGBM, HistGradientBoosting, and a Simple Decision Tree. Each of these base learners is trained on the geospatial input features  $X$ , producing class probability estimates  $p_i^{(y|x)}$ . Second, these outputs are concatenated with the original geospatial features to construct enriched meta-features  $Z = [X, p_1, p_2, p_3]$ . This design preserves raw input information while integrating the predictive strengths and diversity of the base models, allowing the meta-layer to capture higher-order relationships. Finally, a regularized logistic regression model serves as the meta-learner, estimating the susceptibility probability through  $\hat{y} = \sigma(w^T Z + b)$ , where  $w$  are the learned weights reflecting the relative reliability of each base learner and input feature,  $b$  is the bias term, and  $\sigma(\cdot)$  is the sigmoid function ensuring calibrated probabilities. Regularization (L1/L2 penalty) prevents overfitting by constraining the weight magnitudes, encouraging stable generalization across diverse landscapes.

## 2.5 Validation methods

The validation framework employs a comprehensive set of metrics to evaluate model performance, including F1 score, Overall Accuracy, AUC (Area Under the ROC Curve), and Recall, which provide complementary insights into different aspects of classification performance. F1 score offers a balanced

measure of precision and recall, while Overall Accuracy provides a general assessment of correct classifications. The AUC evaluates the model ability to distinguish between classes across all possible thresholds, and Recall measures the proportion of actual positive instances correctly identified. For detailed mathematical formulations and technical specifications of these metrics, please refer to the paper methodology section.

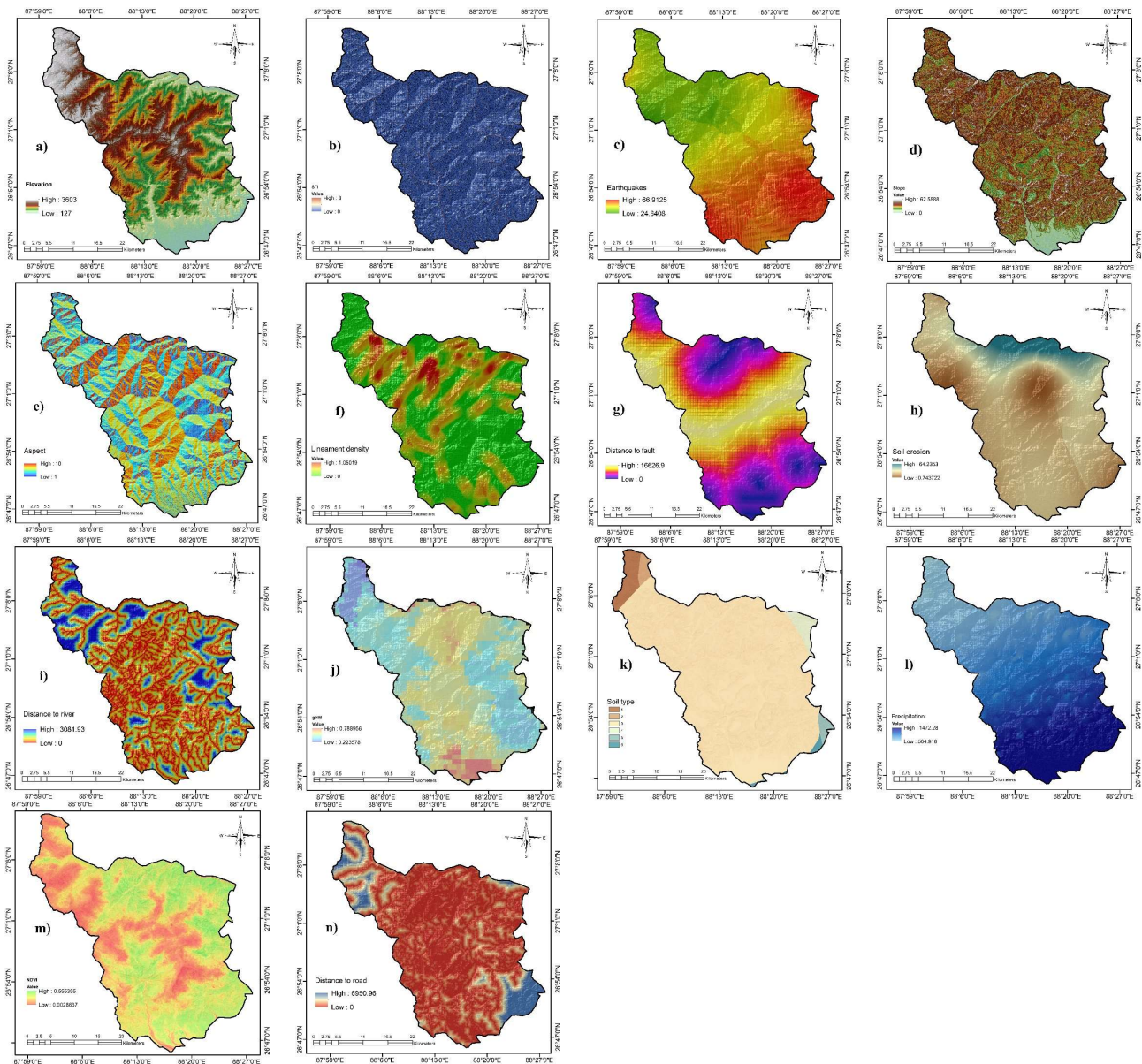


**Figure 4.** Landslide influencing factors: (a) elevation, (b) STI, (c) earthquakes, (d) slope, (e) aspect, (f) lineament density, (g) distance to fault, (h) soil erosion, (i) distance to river, and (j) GHM, (k) soil type, (l) precipitation, (m) NDVI, and (n) distance to road.

## 3. RESULT AND DISCUSSIONS

### 3.1 Correlation Analysis

The feature correlation matrix highlights key relationships among landslide factors: strong negative correlations between elevation and both precipitation ( $r = -0.68$ ) and NDVI ( $r = -0.73$ ) indicate reduced rainfall and vegetation at higher altitudes; a strong positive link between precipitation and earthquakes ( $r = 0.87$ ) suggests possible hydroseismic interactions; and moderate correlations between NDVI and soil erosion ( $r = 0.40$ ) underscore

vegetation's stabilizing role. Negative elevation–road distance correlation ( $r = -0.37$ ) reflects valley-based infrastructure patterns. Weak correlations ( $|r| < 0.20$ ) for variables like aspect and lineament density justify nonlinear modeling. These interdependencies informed feature selection to reduce multicollinearity while retaining geomorphologically relevant predictors (Figure 5).

### 3.2 Feature Importance Analysis

The RF feature importance analysis identified slope gradient (0.28) as the most critical determinant of landslide susceptibility, followed by human modification (GHM; 0.089), proximity to faults (0.087), and elevation (0.085). Precipitation (0.071), seismic activity (0.061), and road proximity (0.059) exhibited moderate influence, while hydrologic (STI: 0.059) and vegetation-related factors (NDVI: 0.054) showed comparatively lower contributions. Notably, soil characteristics (erosion: 0.051; type: 0.008) and lineament density (0.032) had minimum predictive relevance (Figure 5).

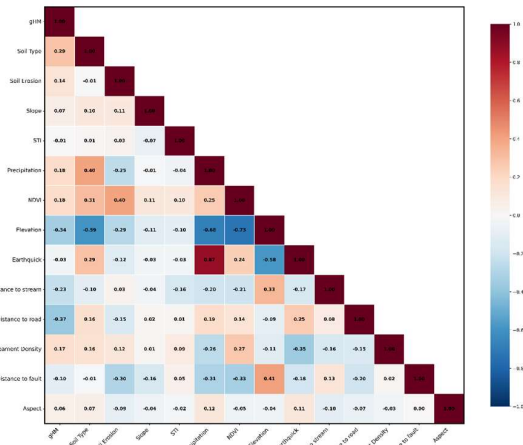


Figure 5. Correlation matrix of landslide conditioning factors.

These results underscore the dominance of topographic (slope, elevation) and geologic (fault proximity) factors over hydrologic or vegetation controls in governing landslide susceptibility (Figure 6).

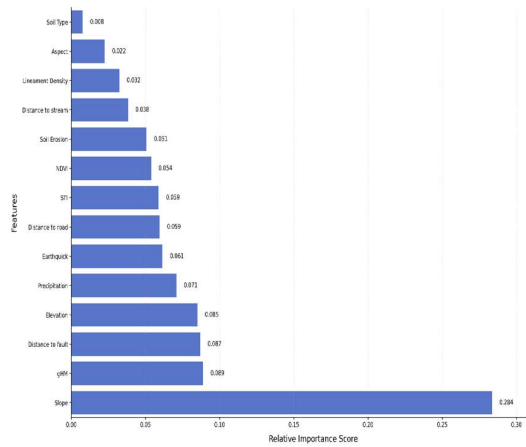
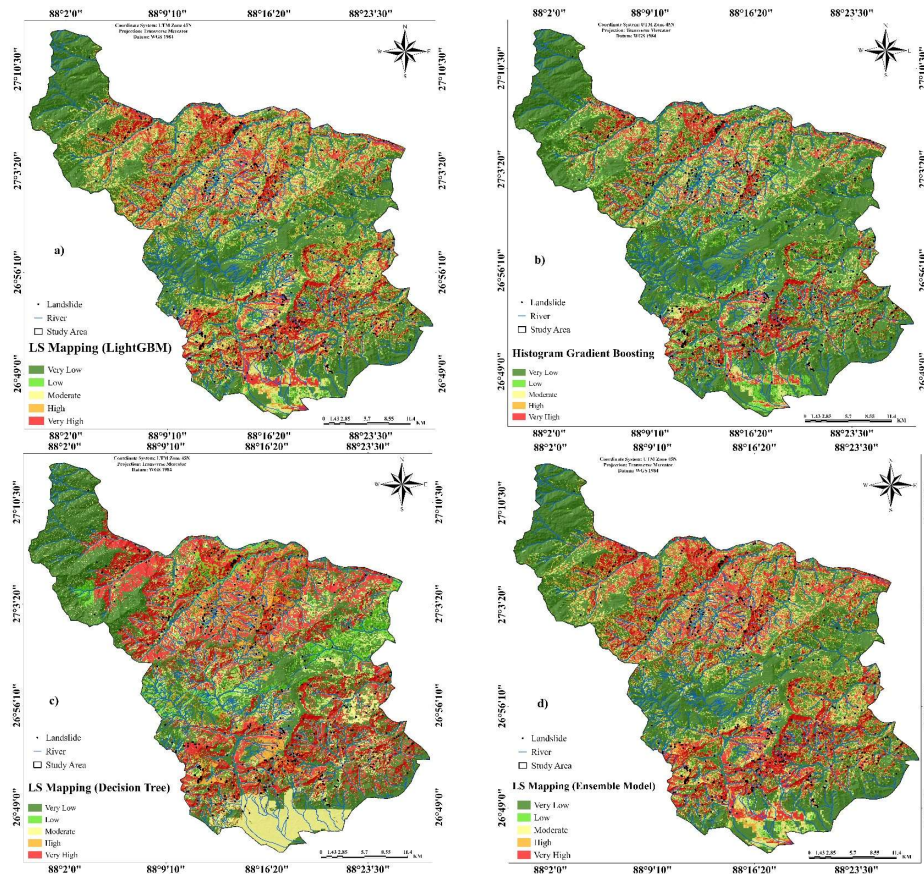


Figure 6. Relative importance of landslide conditioning factors as determined by RF analysis.

### 3.3 Landslide Susceptibility Mapping

The LSMs generated by the proposed Meta-Stacking Ensemble, LightGBM, Histogram Gradient Boosting, and DT models were classified into five risk categories, namely very low, low, moderate, high, and very high (Figures 7 and 8). The results demonstrate distinct distribution patterns across the models.



**Figure 7.** Landslide susceptibility map using (a) LightGBM, (b) Histogram Gradient Boosting, (c) DT, and (d) Proposed Meta-Stacking Ensemble model.

### 3.4 Landslide Susceptibility Mapping

The LSMs generated by the proposed Meta-Stacking Ensemble, LightGBM, Histogram Gradient Boosting, and DT models were classified into five risk categories, namely very low, low, moderate, high, and very high (Figures 7 and 8). The results demonstrate distinct distribution patterns across the models. The results reveals critical insights into how each model prioritizes landslide risk zones. The proposed Meta-Stacking Ensemble demonstrates a balanced distribution, with 40% of the area classified as "Very Low" and 22% as "Very High," suggesting it effectively captures both stable and high-risk regions without extreme biases. In contrast, Histogram Gradient Boosting shows a conservative approach, assigning 55% of the area to "Very Low" susceptibility, the highest among all models, but only 13% to "Very High," potentially underestimating risk zones. LightGBM strikes a middle ground, with 45% "Very Low" and 16% "Very High," while the Decision Tree exhibits polarizing behavior, allocating the lowest "Low" risk coverage (8%) but the highest "Very High" (25%), indicating potential overfitting or sensitivity to localized features. These disparities highlight the inherent trade-offs between model complexity and risk interpretation, with the ensemble model providing a more robust and generalizable solution for LSM.

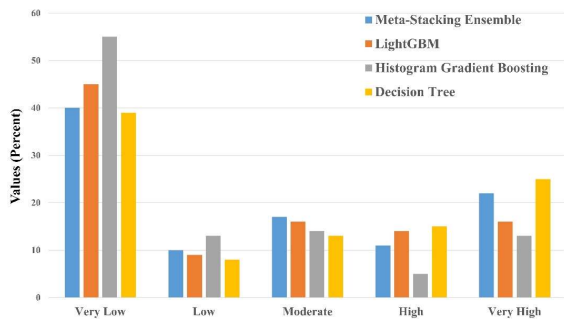


**Figure 8.** Distribution of landslide susceptibility categories across modelling approaches.

### 3.5 Comparison of Validation Methods

Table 1 compares the predictive performance of the LightGBM, Hist Gradient Boosting, DT, and the proposed Meta-Stacking Ensemble models on the test datasets. The Meta-Stacking Ensemble achieved the highest scores across all metrics, with an AUC of 0.93, an F1-score of 0.72, a recall of 0.84, and an overall accuracy of 0.87. LightGBM also performed well, closely followed by Hist Gradient Boosting, while DT exhibited the lowest performance among the evaluated models. According to AUC values, the RRF model had the better predictive performance compared to that of the NB model (Figure 9).

Parameters / Models	LightGBM	Hist Gradient Boosting	DT	Meta-Stacking Ensemble
<b>AUC</b>	<b>0.90</b>	<b>0.89</b>	<b>0.83</b>	<b>0.93</b>
<b>F1</b>	<b>0.70</b>	<b>0.68</b>	<b>0.62</b>	<b>0.72</b>
<b>Recall</b>	<b>0.82</b>	<b>0.80</b>	<b>0.65</b>	<b>0.84</b>
<b>OA</b>	<b>0.84</b>	<b>0.85</b>	<b>0.80</b>	<b>0.87</b>

**Table 1.** Validation results of ML models for landslide susceptibility prediction.

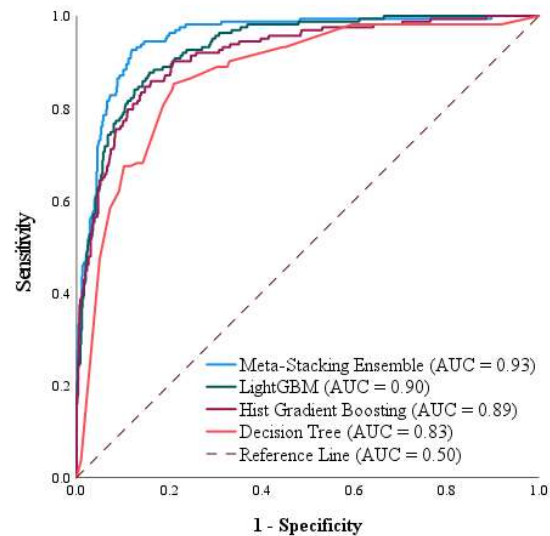


**Figure 9.** Receiver operating characteristic (ROC) curves comparing model performance.

## 4. CONCLUSION AND RECOMMENDATIONS

Landslides represent one of the most destructive natural hazards in mountainous regions like the Darjeeling Himalayas, requiring advanced predictive models for effective risk management. This study developed a novel Meta-Stacking Ensemble model to overcome the limitations of traditional ML approaches in LSM. By integrating LightGBM, Hist Gradient Boosting, and Decision Tree algorithms with a regularized logistic regression meta-learner, the proposed framework preserved critical geo-environmental features during meta-training while maximizing error diversity among base models. This innovative architecture addressed three key challenges including loss of spatial information in conventional stacking methods, correlated errors in homogeneous ensembles, and computational inefficiency in deep learning models.

The results demonstrated the proposed model superior predictive capability, achieving an AUC of 0.93, F1-score of 0.72, and overall accuracy of 87%, outperforming both its base models (e.g., LightGBM: AUC = 0.91; DT: AUC = 0.85) and existing methods like Fuzzy-AHP (AUC = 0.87). Feature importance analysis revealed that slope (28%) was the most influential factor, whereas aspect and soil type had negligible impacts. Spatially, the proposed ensemble susceptibility map classified 22% of the study area as "Very High" risk, with balanced distributions across other risk categories. This contrasted with standalone models; for instance, the DT overestimated high-risk zones (25% "Very High"), while Hist Gradient Boosting exhibited excessive caution (55% "Very Low").

The proposed framework generates GIS-compatible susceptibility maps that enable authorities to implement targeted risk reduction measures. These outputs support evidence-based land-use planning and early warning systems in vulnerable regions. Future work could incorporate higher-resolution data and real-time monitoring to improve predictions. This approach offers a practical framework for landslide risk management in mountainous areas worldwide.

## REFERENCES

- Agboola, G., Beni, L.H., Elbayoumi, T., Thompson, G., 2024. Optimizing landslide susceptibility mapping using machine learning and geospatial techniques. *Ecological Informatics* 81, 102583. <https://doi.org/10.1016/j.ecoinf.2024.102583>
- Banerjee, S., Biswas, C.S., Pal, M., Biswas, S., Hossain, Md.G., Bharti, P., 2022. REPORTED CASES IPC CRIMES AGAINST CHILDREN IN WEST BENGAL, INDIA: A STUDY WITH RECENT DATA. *International Journal of Social Sciences & Economic Environment* 7, 27–40. <https://doi.org/10.53882/ijssce.2022.0701004>
- Barman, J., Biswas, B., Das, J., 2022a. Mizoram, the Capital of Landslide: A Review of Articles Published on Landslides in Mizoram, India. *Monitoring and Managing Multi-hazards: A Multidisciplinary Approach* 97–104.
- Barman, J., Soren, D.D.L., Biswas, B., 2022b. Landslide Susceptibility Evaluation and Analysis: A Review on Articles Published During 2000 to 2020. *Monitoring and Managing Multi-hazards: A Multidisciplinary Approach* 211–220.
- Basharat, M. ul, Khan, J.A., Abdo, H.G., Almohamad, H., 2023. An integrated approach based landslide susceptibility mapping: case of Muzaffarabad region, Pakistan. *Geomatics, Natural Hazards and Risk* 14. <https://doi.org/10.1080/19475705.2023.2210255>
- Bera, S., Upadhyay, V.K., Guru, B., Oommen, T., 2021. Landslide inventory and susceptibility models considering the landslide typology using deep learning: Himalayas, India. *Natural Hazards* 108, 1257–1289. <https://doi.org/10.1007/s11069-021-04731-8>
- Biswas, B., Rahaman, A., Barman, J., 2023. Comparative Assessment of FR and AHP Models for Landslide Susceptibility Mapping for Sikkim, India and Preparation of Suitable Mitigation Techniques. *J Geol Soc India* 99, 791–801. <https://doi.org/10.1007/s12594-023-2386-x>
- Chawla, A., Pasupuleti, S., Chawla, S., Rao, A.C.S., Sarkar, K., Dwivedi, R., 2019. Landslide Susceptibility Zonation Mapping: A Case Study from Darjeeling District, Eastern Himalayas, India. *Journal of the Indian Society of Remote Sensing* 47, 497–511. <https://doi.org/10.1007/s12524-018-0916-6>
- Chu, L., Oloo, F., Bergstedt, H., Blaschke, T., 2020. Assessing the Link between Human Modification and Changes in Land Surface Temperature in Hainan, China Using Image Archives from Google Earth Engine. *Remote Sensing* 12, 888. <https://doi.org/10.3390/rs12050888>
- Csáfordi, P., Pödör, A., Bug, J., Gribovsyki, Z., 2012. Soil Erosion Analysis in a Small Forested Catchment Supported by ArcGIS Model Builder. *Acta Silvatica et Lignaria Hungarica* 8 (2012), Nr. 1 8, 39–56. <https://doi.org/10.15488/259>
- Farhadi, Z., Bevrani, H., Feizi-Derakhshi, M.-R., Kim, W., Ijaz, M.F., 2022. An Ensemble Framework to Improve the Accuracy of Prediction Using Clustered Random-Forest and Shrinkage Methods. *Applied Sciences* 12, 10608. <https://doi.org/10.3390/app122010608>
- Gupta, S.K., Shukla, D.P., 2022. Effect of scale and mapping unit on landslide susceptibility mapping of Mandakini River Basin, Uttarakhand, India. *Environmental Earth Sciences* 81. <https://doi.org/10.1007/s12665-022-10487-6>
- Gupta, V., Paul, A., Kumar, S., Dash, B., 2021. Spatial Distribution of Landslides Vis-à-Vis Epicentral Distribution of Earthquakes in The Vicinity of The Main Central Thrust Zone, Uttarakhand Himalaya, India. *Current Science* 120, 1927–1932. <https://doi.org/10.18520/cs/v120/i12/1927-1932>
- Habibi, A., Delavar, M., Sadeghian, M., Nazari, B., 2022. Chi-square automatic interaction detection (CHAID) algorithm for flood susceptibility assessment in Sardabroud watershed, Iran.
- Habibi, Alireza, Delavar, M.R., Nazari, B., Pirasteh, S., Sadeghian, M.S., 2023a. A novel approach for flood hazard assessment using hybridized ensemble models and feature selection algorithms. *International Journal of Applied Earth Observation and Geoinformation* 122, 103443. <https://doi.org/10.1016/j.jag.2023.103443>
- Habibi, A., Delavar, M.R., Sadeghian, M.S., Nazari, B., 2023. FLOOD SUSCEPTIBILITY MAPPING AND ASSESSMENT USING REGULARIZED RANDOM FOREST AND NAÏVE BAYES ALGORITHMS, in: ISPRS Annals of the Photogrammetry, Remote Sensing and Spatial Information Sciences. Presented at the ISPRS WG IV/3<br>ISPRS GeoSpatial Conference 2022, Joint 6th Sensors and Models in Photogrammetry and Remote Sensing (SMPR) and 4th Geospatial Information Research (GIResearch) Conferences - 19&ndash;22 February 2023, Tehran, Iran (virtual), Copernicus GmbH, pp. 241–248. <https://doi.org/10.5194/isprs-annals-X-4-W1-2022-241-2023>
- Habibi, Alireza, Delavar, M.R., Sadeghian, M.S., Nazari, B., Pirasteh, S., 2023b. A hybrid of ensemble machine learning models with RFE and Boruta wrapper-based algorithms for flash flood susceptibility assessment. *International Journal of Applied Earth Observation and Geoinformation* 122, 103401. <https://doi.org/10.1016/j.jag.2023.103401>
- Höge, M., Scheidegger, A., Baity-Jesi, M., Albert, C., Fenicia, F., 2022. Improving hydrologic models for predictions and process understanding using neural ODEs. *Hydrology and Earth System Sciences* 26, 5085–5102. <https://doi.org/10.5194/hess-26-5085-2022>
- Jakob, M., 2022. Landslides in a changing climate. *Landslide Hazards, Risks, and Disasters*. <https://doi.org/10.1016/b978-0-12-818464-6.00003-2>
- Kim, G.I., Kim, S., Jang, B., 2023. Classification of mathematical test questions using machine learning on datasets of learning management system questions. *PLoS One* 18, e0286989. <https://doi.org/10.1371/journal.pone.0286989>
- Lee, S., Lee, M.-J., Jung, H.-S., 2017. Data Mining Approaches for Landslide Susceptibility Mapping in Umyeonsan, Seoul, South Korea. *Applied Sciences* 7, 683. <https://doi.org/10.3390/app7070683>
- Moghimi, A., Singha, C., Fathi, M., Pirasteh, S., Mohammadzadeh, A., Varshosaz, M., Huang, J., Li, H., 2024. Hybridizing genetic random forest and self-attention based CNN-LSTM algorithms for landslide susceptibility mapping in Darjiling and Kurseong, India. *Quaternary Science Advances* 14, 100187. <https://doi.org/10.1016/j.qsa.2024.100187>

- Naceur, H.A., Abdo, H.G., Igmoullan, B., Namous, M., Almohamad, H., Al Dughairi, A.A., Al-Mutiry, M., 2022. Performance assessment of the landslide susceptibility modelling using the support vector machine, radial basis function network, and weight of evidence models in the N'fis river basin, Morocco. *Geoscience Letters* 9. <https://doi.org/10.1186/s40562-022-00249-4>
- Pawde, M.B., Saha, S.S., 1982. *Geology of the Darjeeling Himalaya*. Miscellaneous publication-Geological survey of India 50–55.
- Peethambaran, B., Anbalagan, R., Shihabudheen, K. V., 2018. Landslide susceptibility mapping in and around Mussoorie Township using fuzzy set procedure, MamLand and improved fuzzy expert system-A comparative study. *Natural Hazards* 96, 121–147. <https://doi.org/10.1007/s11069-018-3532-4>
- Roy, J., Saha, S., 2019. Landslide susceptibility mapping using knowledge driven statistical models in Darjeeling District, West Bengal, India. *Geoenviron Disasters* 6, 1–18. <https://doi.org/10.1186/s40677-019-0126-8>
- Saha, S., Majumdar, P., Bera, B., 2023. Deep learning and benchmark machine learning based landslide susceptibility investigation, Garhwal Himalaya (India). *Quaternary Science Advances* 10, 100075. <https://doi.org/10.1016/j.qsa.2023.100075>
- Saha, S., Roy, J., Hembram, T.K., Pradhan, B., Dikshit, A., Abdul Maulud, K.N., Alamri, A.M., 2021. Comparison between Deep Learning and Tree-Based Machine Learning Approaches for Landslide Susceptibility Mapping. *Water* 13, 2664. <https://doi.org/10.3390/w13192664>
- Sarkar, S., Roy, A.K., Martha, T.R., 2013. Landslide susceptibility assessment using information value method in parts of the Darjeeling Himalayas. *Journal of the Geological Society of India* 82, 351–362.
- Shao, X., Xu, C., 2022. Earthquake-induced landslides susceptibility assessment: A review of the state-of-the-art. *Natural Hazards Research* 2, 172–182. <https://doi.org/10.1016/j.nhres.2022.03.002>
- Sonker, I., Tripathi, J.N., Singh, A.K., 2021. Landslide susceptibility zonation using geospatial technique and analytical hierarchy process in Sikkim Himalaya. *Quaternary Science Advances* 4, 100039. <https://doi.org/10.1016/j.qsa.2021.100039>
- Starkel, L., Basu, S., 2000. Rains, landslides, and floods in the Darjeeling Himalaya.
- Sumantra, S.B., Raghunath, P., 2016. Causes of Landslides in Darjeeling Himalayas during June-July, 2015. *J Geogr Nat Disasters* 6, 1–5.
- Yi, Y., Zhang, W., Xu, X., Zhang, Z., Wu, X., 2022. Evaluation of neural network models for landslide susceptibility assessment. *International Journal of Digital Earth* 15, 934–953. <https://doi.org/10.1080/17538947.2022.2062467>
- Yi, Y., Zhang, Z., Zhang, W., Jia, H., Zhang, J., 2020. Landslide susceptibility mapping using multiscale sampling strategy and convolutional neural network: A case study in Jiuzhaigou region. *CATENA* 195, 104851. <https://doi.org/10.1016/j.catena.2020.104851>
- Youssef, A.M., Pradhan, B., Dikshit, A., Al-Katheri, M.M., Matar, S.S., Mahdi, A.M., 2022. Landslide susceptibility mapping using CNN-1D and 2D deep learning algorithms: comparison of their performance at Asir Region, KSA. *Bulletin of Engineering Geology and the Environment* 81. <https://doi.org/10.1007/s10064-022-02657-4>
- Zhang, S., Bai, L., Li, Y., Li, W., Xie, M., 2022. Comparing Convolutional Neural Network and Machine Learning Models in Landslide Susceptibility Mapping: A Case Study in Wenchuan County. *Frontiers in Environmental Science* 10. <https://doi.org/10.3389/fenvs.2022.886841>
- Zhu, L., Huang, L., Fan, L., Huang, J., Huang, F., Chen, J., Zhang, Z., Wang, Y., 2020. Landslide Susceptibility Prediction Modeling Based on Remote Sensing and a Novel Deep Learning Algorithm of a Cascade-Parallel Recurrent Neural Network. *Sensors (Basel, Switzerland)* 20, 1576. <https://doi.org/10.3390/s20061576>